



# Deprotonation and dehydrogenation of Di(2-pyridylmethyl)amine with $M\{N(SiMe_3)_2\}_2$ ( $M = Mn, Fe, Co, Zn$ ) and $Fe(C_6H_2-2,4,6-Me_3)_2$

Astrid Malassa, Christine Agthe, Helmar Görls, Manfred Friedrich, Matthias Westerhausen\*

Institut für Anorganische und Analytische Chemie, Friedrich-Schiller-Universität Jena, August-Bebel-Str. 2, D-07743 Jena, Germany

## ARTICLE INFO

### Article history:

Received 26 February 2010

Received in revised form

30 March 2010

Accepted 4 April 2010

Available online 21 April 2010

### Keywords:

Deprotonation reactions

Azaallyl ligands

Metallation reactions

Transamination reactions

Redox reactions

Dehydrogenation reactions

## ABSTRACT

The reaction of di(2-pyridylmethyl)amine with  $FeCl_2$  yields  $[Fe\{HN(CH_2Py)_2\}_2]Cl_2$  (**1**) with the tridentate amines coordinating in a facial manner at the iron(II) center. Transamination of this amine with  $[M\{N(SiMe_3)_2\}_2]$  in an equimolar ratio leads to the formation of heteroleptic  $[(Me_3Si)_2N-M\{\mu-N(CH_2Py)_2\}_2]$  [ $M = Mn$  (**2a**),  $Fe$  (**2b**), and  $Zn$  (**2c**)]. The metallation of di(2-pyridylmethyl)amine with dimesityl iron(II) gives  $[Mes-Fe\{\mu-N(CH_2Py)_2\}_2]$  (**3**). At temperatures below  $-30^\circ C$  the transamination reaction of  $[Fe\{N(SiMe_3)_2\}_2]$  with di(2-pyridylmethyl)amine in a molar ratio of 1:2 yields  $[Fe\{N(CH_2Py)_2\}_2]$  (**4**). The reaction of  $[Co\{N(SiMe_3)_2\}_2]$  with  $HN(CH_2Py)_2$  leads to the formation of  $[Co\{N(CH_2Py)_2\}_2]$  (**5b**) with 1,3-di(2-pyridyl)-2-azaallyl ligands, regardless of the employed stoichiometry. The compounds **2b**, **2c**, **3**, and **4** have to be handled and manipulated at low temperatures because they degrade already at room temperature whereas the manganese(II) derivative **2a** is stable under these conditions. The degradation products  $[M\{N(CH_2Py)_2\}_2]$  [ $M = Fe$  (**5a**),  $Zn$  (**5c**)] contain the 1,3-di(2-pyridyl)-2-azaallyl ligands and can be considered as the dehydrogenation products of  $[M\{N(CH_2Py)_2\}_2]$ . A metathetical approach via the reaction of lithium di(2-pyridylmethyl)amide with  $FeCl_2$  did not give the desired product **4** but a mixture of **1** and **5a**. A  $^1H$  NMR and EPR spectroscopic pursuit of the degradation of  $[(Me_3Si)_2N-Zn\{\mu-N(CH_2Py)_2\}_2]$  (**2c**) in tetrahydrofuran at temperatures between 253 and 328 K showed diminishing amounts of **2c** and the appearance of 1,3-di(2-pyridyl)-2-azaallyl anions whereas the EPR experiments clearly verify the presence of di(2-pyridylmethyl)aminyl radicals in solution.

© 2010 Elsevier B.V. All rights reserved.

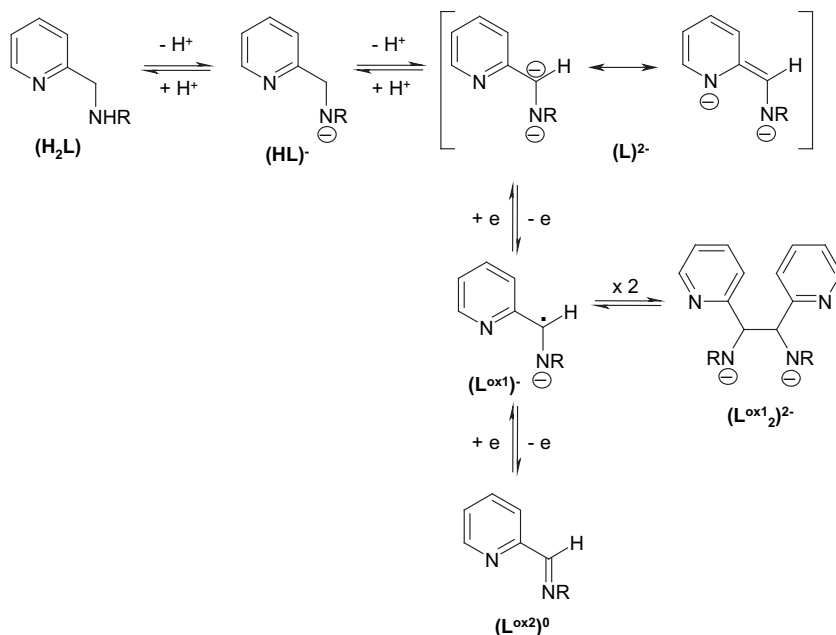
## 1. Introduction

2-Pyridylmethylamines (abbreviated in Scheme 1 as  $H_2L$ ) offer a rich chemistry including deprotonation (amide formation) as well as redox reactions (imine formation). In Scheme 1 possible pathways are summarized. Single and double deprotonations of ( $H_2L$ ) lead to the formation of amides ( $HL$ )<sup>-</sup> (deprotonation of the amino group) and bisamides ( $L$ )<sup>2-</sup> (deprotonation at the methylene fragment and delocalization of the anionic charge into the pyridyl unit), respectively. Whereas the amides ( $HL$ )<sup>-</sup> represent widely used ligands, the doubly metallated amines are only stable as salts with cations of very electropositive metals such as lithium [1] and magnesium [2]. Nobler metals such as tin(II) and zinc(II) initiate a single electron transfer reaction yielding the radical anion ( $L^{ox1}$ )<sup>-</sup>, which can dimerize to C–C coupled ( $L^{ox1_2}$ )<sup>2-</sup>, and elemental metal. If R represents an alkyl group the dimerization

is reversible [3–6] whereas with  $R = SiR'_3$  only the C–C coupled dimer was observed [2,7]. Iron(III) compounds are even able to doubly oxidize the amides leading to the imines ( $L^{ox2}$ )<sup>0</sup> which form adducts with the iron(II) cations [8]. The imine ( $L^{ox2}$ )<sup>0</sup> ( $R = H$ ) formed also from the reaction of cobalt(III) with 2-pyridylmethylamine ( $H_2L$ ) ( $R = H$ ) in anaerobic basic aqueous solutions [9]; the proposed mechanism for the oxidative dehydrogenation of the amine ( $H_2L$ ) to ( $L^{ox2}$ )<sup>0</sup> included unobserved intermediates which could be considered as ( $HL^{ox1}$ ) and ( $HL^{ox2}$ )<sup>+</sup>; the latter was finally deprotonated by  $OH^-$  anions. However, the aerial oxidation of cobalt(II)-bound 2-pyridylmethylamine ( $R = H$ ) was explained by oxidation of ( $H_2L$ ) with air yielding an intermediate of the type ( $H_2L^{ox1}$ )<sup>+</sup> which can be deprotonated. If deprotonation occurs at the methylene unit a C–C coupling reaction could follow yielding 1,2-diamino-1,2-di(2-pyridyl)ethane  $H_2(L^{ox1_2})$  [10]. Subsequent reaction sequences lead to isolated heterocycles. In general, the small substituent  $R = H$  can lead to various side-products [11] whereas trialkylsilyl groups at the amido functionality allow an easier control of the reaction behaviour of these amides. The reduction of ( $L^{ox2}$ ) with

\* Corresponding author. Tel.: +49 3641 948110; fax: +49 3641 948102.

E-mail addresses: m.we@uni-jena.de, m.we@uni-jena.de (M. Westerhausen).

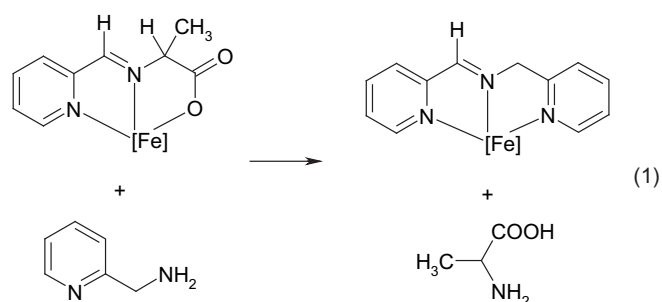


**Scheme 1.** Reaction portfolio starting from 2-pyridylmethylamine. Proton transfer reactions (acid–base reactions) are shown within rows, electron transfer reactions (redox reactions) are shown within columns.

sodium gives the anions  $(L^{ox1})^-$  which can be coordinated to metal(II) atoms such as Cr, Mn, Fe, Co, Ni, and Zn [12]. These transition metal complexes show no tendency to dimerize via a C–C coupling reaction.

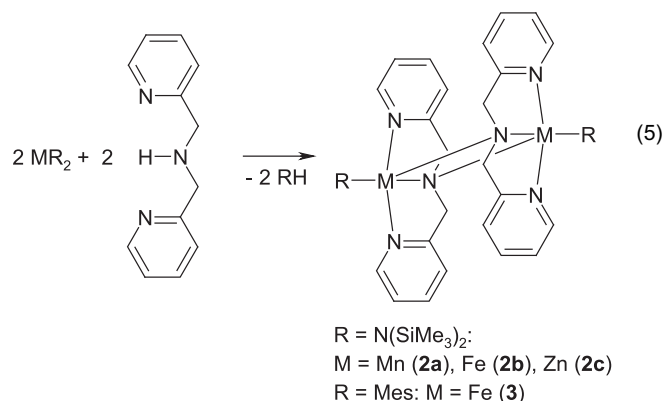
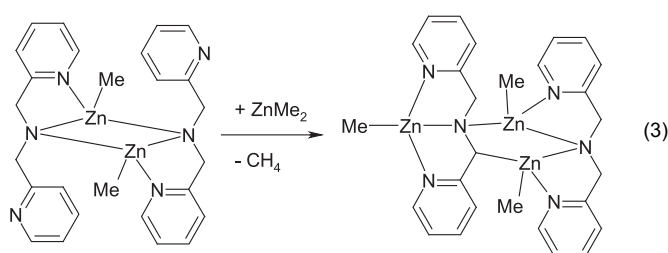
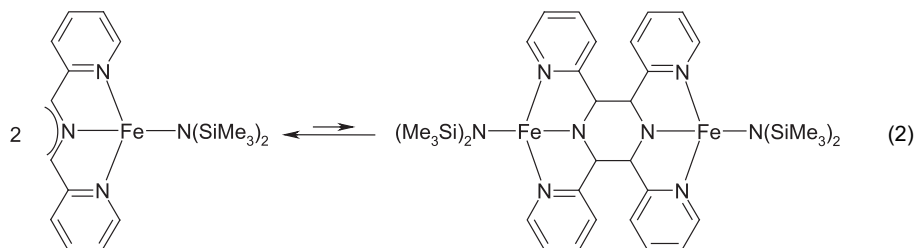
Whereas in Scheme 1 the amino-bound group R remained an innocent substituent, this is not the case if R is another 2-pyridylmethyl group. Iron(II) complexes with coordinated di(2-pyridylmethyl)amine molecules are well-known for several decades. These ligands are stable toward oxidation even in the coordination sphere of iron(III) and under aerobic conditions [13]. Several of these iron(II) complexes with different counter anions have been characterized by X-ray structure determinations and show an octahedrally surrounded iron(II) center with a facial arrangement of the tridentate ligands, counter ions being e.g. chlorides [13] or bromides [14]. The formation of dialkylamides is far less common for the late 3d transition metals from Mn to Cu. Dialkylamides act as two-electron  $\sigma$  donors but they are also in the position to act as two-electron  $\pi$  donors, and therefore they favor complex formation with early transition metals which have vacant d orbitals and act as  $\pi$  acceptor metals [15,16]. However, an increasing interest in these compounds led to vast development of the amide chemistry also of the late transition metals, employing electronic and steric protection [17]. In contrast to the finding that dialkylamides of manganese(II), iron(II), and cobalt (II) are difficult to prepare and handle, the homoleptic bis(trimethylsilyl)amides of these late 3d metals Mn [18–20], Fe [20–22], and Co [19,20,22] are stable and therefore they often serve as starting materials in metallation and transamination reactions.

Dehydrogenation of di(2-pyridylmethyl)amine yields  $Py-CH_2-N=CH-Py$  (which, of course, could be understood as a sequence of two deprotonation and two oxidation steps) but this imine can easily be prepared from 2-pyridylcarbaldehyde and 2-pyridylmethylamine, too [23]. This ligand was also synthesized in the coordination sphere of iron(II) according to equation (1) where [Fe] represents a complex fragment of iron(II) [24]. Spectroscopic investigations of  $[Fe(Py-CH_2-N=CH-Py)_2]^{2+}$  with perchlorate counter ions showed a strong  $\sigma$ -bonding ligand [25].



Lithiation of  $Py-CH_2-N=CH-Py$  and reaction with metal(II) salts such as  $(thf)_2FeBr_2$ ,  $CoCl_2$ , and  $(dme)NiCl_2$  yielded the bis[1,3-di(2-pyridyl)-2-azaallyl] derivatives of iron, cobalt, and nickel. In addition a direct metallation of  $Py-CH_2-N=CH-Py$  with  $(thf)Fe[N(SiMe_3)_2]_2$  also gave this iron(II) derivative [26]. Thermal degradation of methylzinc di(2-pyridylmethyl)amide led to the formation of bis[1,3-di(2-pyridyl)-2-azaallyl] zinc [27]. However, heteroleptic 1,3-di(2-pyridyl)-2-azaallyl iron(II) bis(trimethylsilyl)amide shows an equilibrium with the C–C coupled dimer as shown in equation (2) [26]. A similar C–C-coupled bridging hexadentate azabase was already detected as a zinc complex from the reaction of 2-pyridylmethylamine with excess of dimethylzinc [11].

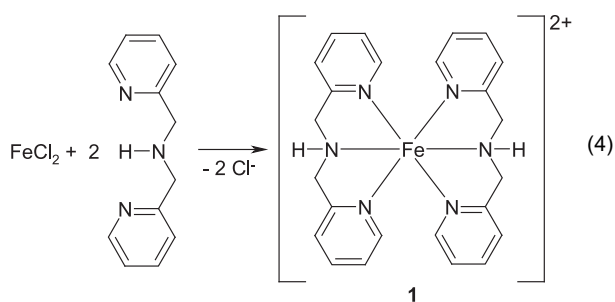
First experiments showed that a dimethylzinc-mediated intermolecular deprotonation of methylzinc di(2-pyridylmethyl)amide allowed the isolation of a trinuclear zinc complex as shown in equation (3) [28]. We investigated the metallation of di(2-pyridylmethyl)amine with the bis(trimethylsilyl)amides of manganese (II), iron(II), cobalt(II), and zinc(II) (transamination reactions) as well as with dimesityl iron(II). The transamination of N-substituted 2-pyridylmethylamines with  $M[N(SiMe_3)_2]_2$  was already successfully employed to prepare homoleptic bis(2-pyridylmethyl)amides of Mg, Mn, Fe, Co, and Zn [29]. A heteroleptic complex was isolated after the reaction of lithium 2-pyridylmethylamide with an equimolar amount of  $(thf)_2FeCl_2$ .



## 2. Results and discussion

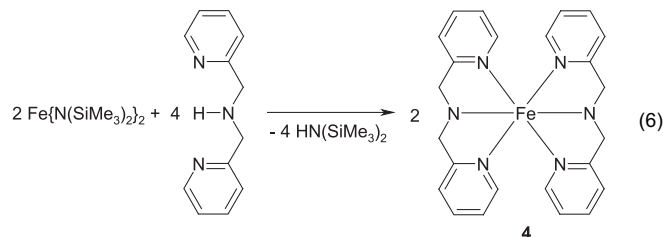
### 2.1. Synthesis

Di(2-pyridylmethyl)amine acts as a tridentate ligand at iron(II). The reaction of this amine with iron(II) chloride in dichloromethane led to the formation of  $[\text{Fe}\{\text{HN}(\text{CH}_2\text{Py})_2\}_2]\text{Cl}_2$ . (equation (4)).



The transamination reaction of the metal bis[bis(trimethylsilyl)amides] of manganese, iron, and zinc [30] with di(2-pyridylmethyl)amine in an equimolar ratio yielded the corresponding heteroleptic dimeric complexes  $[(\text{Me}_3\text{Si})_2\text{N-M-N}(\text{CH}_2\text{Py})_2]_2$  [ $M = \text{Mn}$  (**2a**),  $\text{Fe}$  (**2b**),  $\text{Zn}$  (**2c**)] (equation (5)) which precipitated from the reaction mixtures. A similar deprotonation reaction occurred between dimesityl iron [31] and di(2-pyridylmethyl)amine leading to the formation of  $[\text{Mes-Fe-N}(\text{CH}_2\text{Py})_2]_2$  (**3**). A dimerization into the homoleptic compounds  $\text{MR}_2$  and  $\text{M}\{\text{N}(\text{CH}_2\text{Py})_2\}_2$  was not observed. A heteroleptic amido complex  $[\text{Me-Zn}\{\mu\text{-N}(\text{CH}_2\text{Py})_2\}_2]$  contains a four-membered  $\text{Zn}_2\text{N}_2$  ring with tetra-coordinate zinc atoms [27] because only one pyridyl unit of each ligand was bound to the metal atoms.

The synthesis of homoleptic iron bis[di(2-pyridylmethyl)amide] (**4**) was performed via transamination of  $\text{Fe}\{\text{N}(\text{SiMe}_3)_2\}_2$  with  $\text{HN}(\text{CH}_2\text{Py})_2$  at temperatures below  $-30^\circ\text{C}$  according to equation (6) (see also supplementary information of ref. [26]). This compound precipitated immediately from the reaction solution, thus preventing subsequent degradation reactions. In addition, the iron(II) center is electronically saturated according to the 18-electron rule and sterically shielded thus stabilizing this diamido iron(II) complex.



The compounds **2** and **3** proved to be very reactive and already degraded below room temperature. C-H activation and formation of 1,3-di(2-pyridyl)-2-azaallyl ligands led to the formation of homoleptic  $\text{M}\{\text{N}(\text{CHPy})_2\}_2$  [ $M = \text{Fe}$  (**5a**),  $\text{Zn}$  (**5c**)] (equation (7)). The tridentate ligands show a meridional coordination behaviour. In order to follow this reaction by NMR spectroscopy, the zinc complex **2c** was dissolved in tetrahydrofuran and spectra were recorded during heating of the sample from 253 K to 328 K (Fig. 1). Up to a temperature of 283 K the spectrum remained nearly unchanged and degradation was very slow. Above this temperature the formation of the 1,3-di(2-pyridyl)-2-azaallyl ligand was observed. During heating of the sample the degradation of  $[(\text{Me}_3\text{Si})_2\text{N-Zn-N}(\text{CH}_2\text{Py})_2]_2$  (**2c**) became faster and the intensity

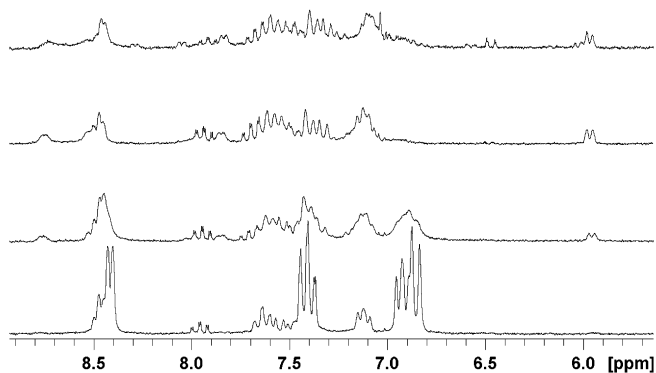
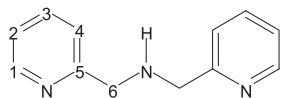


**Fig. 1.** Temperature-dependent  $^1\text{H}$  NMR experiment of the degradation of  $[(\text{Me}_3\text{Si})_2\text{N-Zn}(\mu\text{-N}(\text{CH}_2\text{Py})_2)_2]$  (**2c**) in  $[\text{D}_8]\text{THF}$ . Only the region between 5.7 and 8.9 ppm of aromatic fragments is displayed. From the bottom to the top, the spectra of  $[(\text{Me}_3\text{Si})_2\text{N-Zn}(\mu\text{-N}(\text{CH}_2\text{Py})_2)_2]$  (**2c**) were recorded at 283 K, 300 K, 313 K, and 328 K. The formation of the 1,3-(2-pyridyl)-2-azaallyl anion can best be seen at the appearance of the resonances between 5.7 and 6.7 ppm and at the diminishing resonances of **2c** between 6.8 and 7.0 ppm.

of the resonances between  $\delta = 5.8$  and 6.7 of the 1,3-di(2-pyridyl)-2-azaallyl anions increased. In Table 1 the  $^1\text{H}$  NMR parameters of the involved compounds are listed. The dehydrogenation leads to a strong low field shift of the hydrogen atoms in  $\alpha$ -position to the amido functionality. The first reaction steps involve deprotonation at the methylene units before the azaallyl moieties formed. This fact is in agreement with earlier investigations, shown in equation (3). Other species appear as intermediates in the reaction solution which disappear again at higher temperatures. A repetition of this reaction in an EPR spectrometer showed that also organic radicals play an important role as intermediates (Fig. 2). A simulation of the EPR spectrum reveals that hydrogen abstraction (deprotonation and single electron transfer) leads to the radical  $\text{Py-}\dot{\text{C}}\text{H-N=CH-Py}$  which is stabilized by a far-reaching delocalization of the electron. This delocalization gives rise to intense coupling of the electron with all nitrogen atoms. However, the coupling  $a(\text{N})$  to the pyridyl-nitrogen bases is approximately twice as large as the coupling to the azaallyl N base. This fact is a consequence of the delocalization shown in Scheme 2. A similar observation was made for the  $a(\text{H})$  coupling constants. The largest value can be addressed to the allylic CH moieties. For the pyridyl groups two larger and two smaller

**Table 1**

Comparison of the  $^1\text{H}$  NMR parameters of  $\text{HN}(\text{CH}_2\text{Py})_2$ ,  $[(\text{Me}_3\text{Si})\text{N-Zn-N}(\text{CH}_2\text{Py})_2]$  (**2c**), and  $\text{M}[\text{N}(\text{CHPy})_2]_2$  (**5c**) ( $[\text{D}_8]\text{thf}$  solution, 25 °C, chemical shifts  $\delta$  [ppm], coupling constants  $J$  [Hz]). Numbering scheme:



	$\text{HN}(\text{CH}_2\text{Py})_2$	$[(\text{Me}_3\text{Si})\text{N-Zn-N}(\text{CH}_2\text{Py})_2]$ ( <b>2c</b> )	$\text{M}[\text{N}(\text{CHPy})_2]_2$ ( <b>5c</b> )
$\delta(\text{H1})$	8.47	8.40	7.51
$^3J(\text{H,H})$	4.8	5.0	5.2
$\delta(\text{H2})$	7.11	6.95	6.18
$^3J(\text{H,H})$	5.2	6.3	6.4
$\delta(\text{C3})$	7.62	7.43	7.11
$^3J(\text{H,H})$	7.6	7.6	7.8
$\delta(\text{C4})$	7.42	6.86	6.59
$^3J(\text{H,H})$	8.0	7.8	8.4
$\delta(\text{H6})$	3.89	4.45	7.01
$\delta(\text{NH})$	2.65	—	—

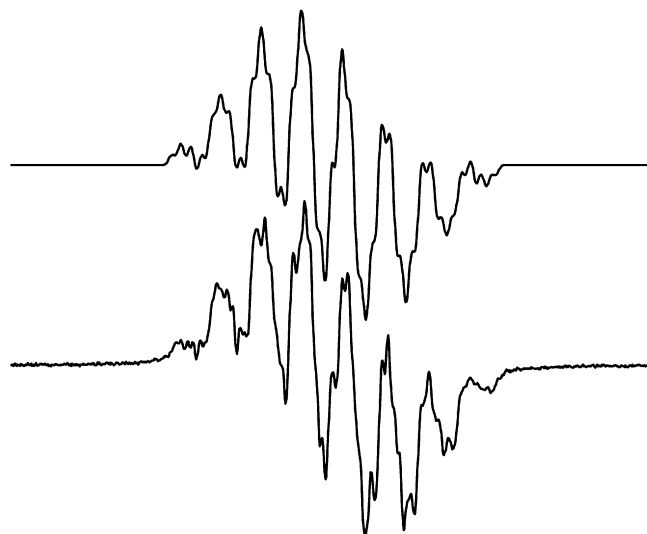
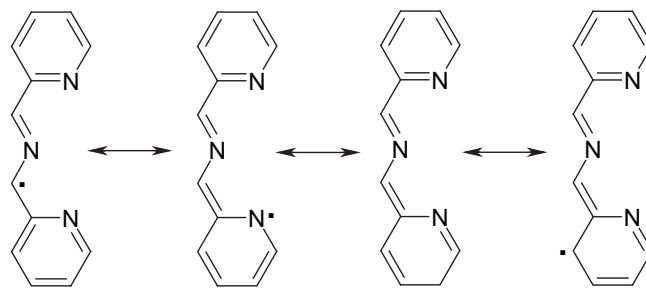


**Fig. 2.** EPR spectrum taken during the degradation of  $[(\text{Me}_3\text{Si})_2\text{N-Zn}(\mu\text{-N}(\text{CH}_2\text{Py})_2)_2]$  (**2c**) leading to the formation of  $[\text{ZnN}(\text{CHPy})_2]_2$  (**5c**) at r.t. ( $[\text{D}_8]\text{THF}$  solution, bottom spectrum). This organic radical was simulated with the following values:  $g = 2.00718$ ,  $a(\text{N}_{\text{amide}}) = 2.19$  G,  $a(\text{N}_{\text{py}}) = 3.97$  G, and  $a(\text{H})$  values of 3.66 G, 1.10 G, 0.70 G, 0.33 G, and 0.12 G (simulated spectrum at the top).

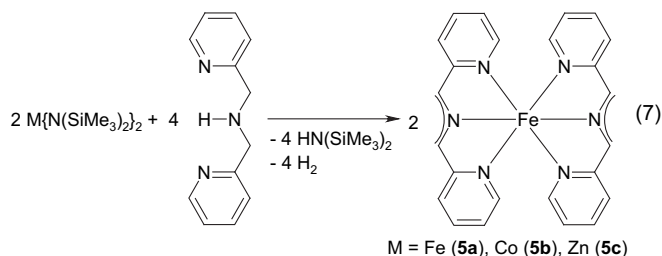


**Scheme 2.** Mesomeric forms of the 1,3-di(2-pyridyl)-2-azaallyl radical showing the delocalization of the radical electron. Similar drawings which are also possible for the other 2-pyridylmethyl group are not represented.

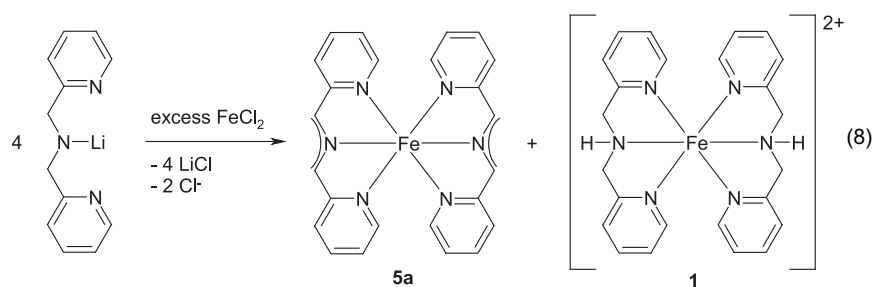
couplings are found which is in agreement with the valence bond formula given in Scheme 2.

The analysis of the space above the solution showed that small amounts of hydrogen gas were liberated from this reaction mixture.

The reaction of cobalt bis[bis(trimethylsilyl)amide] with di(2-pyridylmethyl)amine gave directly cobalt bis[1,3-di(2-pyridyl)-2-azapropenide] (**5b**) and we were unable to isolate intermediate  $[(\text{Me}_3\text{Si})\text{N-Co-N}(\text{CH}_2\text{Py})_2]_2$ . A similar reaction protocol with manganese bis[bis(trimethylsilyl)amide] does not lead to the formation of a 1,3-di(2-pyridyl)-2-azaallyl ligand but to the formation of heteroleptic **2a**.



The addition of lithium di(2-pyridylmethyl)amide to a solution of FeCl<sub>2</sub> yielded a mixture of [Fe{HN(CH<sub>2</sub>Py)<sub>2</sub>}<sub>2</sub>]Cl<sub>2</sub> (**1**) and Fe[N(CHPy)<sub>2</sub>]<sub>2</sub> (**5a**) according to equation (8). However, the expected metathesis product [Fe{N(CH<sub>2</sub>Py)<sub>2</sub>}<sub>2</sub>]<sub>2</sub> (**4**) was not found in the reaction mixture. Nevertheless, this complex **4** might form in the first reaction step. Subsequent reactions with still present lithium amide gave the product mixture via deprotonation (lithiation) and redox active intermediates. In this reaction sequence the di(2-pyridylmethyl)amide ligand acted as a hydrogen donor (leading to the formation of the azaallyl complex **5a**) and at the same time as a proton acceptor which gives the neutral di(2-pyridylmethyl)amine ligand in the coordination sphere of iron(II). From this reaction mixture crystalline [Fe{HN(CH<sub>2</sub>Py)<sub>2</sub>}<sub>2</sub>]Cl<sub>2</sub>·CH<sub>2</sub>Cl<sub>2</sub> (**1**·CH<sub>2</sub>Cl<sub>2</sub>) was isolated after recrystallization from dichloromethane.



## 2.2. Molecular structures

The chemistry offers two interesting series which are worth to be discussed in detail. On the one hand the series of the iron(II) derivatives **1**, **4**, and **5a** with the ligands HN(CH<sub>2</sub>Py)<sub>2</sub> (amino complex), N(CH<sub>2</sub>Py)<sub>2</sub> (amido complex), and N(CHPy)<sub>2</sub> (azaallyl derivative), respectively. In all these compounds iron(II) (3d<sup>6</sup> transition metal cation) is located in a distorted octahedral environment. On the other hand, the heteroleptic complexes of manganese(II) (**2a**), iron(II) (**2b**), and zinc(II) (**2c**) as well as complex **3** offer the possibility to discuss the influence of the size of the

cations as well as the electronic influence of different valence electron counts on structural parameters.

Selected structural parameters of the iron(II) derivatives **1**, **4**, and **5a** are listed in Table 2. The major differences can be expected at the amino/amido functionality. In all complexes the iron atom is in a distorted octahedral environment. In **1** the tridentate ligands bind in a facial fashion whereas in **4** and **5** the ligands show a meridional arrangement. In **1** (Fig. 3) the amino nitrogen atom N2 is in a distorted tetrahedral environment leading to a rather large average N2-C distance of 149.9 pm and a long Fe-N2 bond of 203.1 pm. Deprotonation of the amino group (leading to the amido ligand of **4**, see Fig. 4) also gives a shorter Fe-N2 distance of 200.6 pm due to an additional electrostatic attraction between the Fe cation and the amido anion. A much larger effect is observed for the N2-C bonds (142.3 pm) due to an enhancement of the s-orbital contribution (in **1** the N2 atom is sp<sup>3</sup> hybridized, in **4** a sp<sup>2</sup> hybridization

gives the nearly planar coordination sphere). The strong electrostatic attraction between the amido group and the iron atom leads to a significant elongation of the Fe-N1/N3 bonds to the pyridyl units (**1**: av. Fe-N<sub>Py</sub> 198.7 pm, **4**: 221.4 pm). The negative charge of the azaallyl ligand is delocalized not only within the allyl fragment but short C5-C6 and C7-C8 bonds (av. value 141.2 pm) also suggest a delocalization into the pyridyl units whereas values around 150 pm are characteristic for **1** and **4**. The negative charge leads to short Fe-N bonds to the azaallyl fragment as well as to the pyridyl moieties Table 3.

Cl1

**Table 2**

Selected structural parameters of the iron(II) derivatives **1**, **4**, and **5a** with the ligands HN(CH<sub>2</sub>Py)<sub>2</sub> (amino complex), N(CH<sub>2</sub>Py)<sub>2</sub> (amido complex), and N(CHPy)<sub>2</sub> (azaallyl derivative) (bond lengths [pm] and angles [°]).

	<b>1</b>	<b>4</b>	<b>5a</b>
N1-C1	134,6(5)	134,2(4)	133,9(4)
N1-C5	135,1(5)	133,2(4)	137,2(4)
C1-C2	137,8(5)	136,4(5)	138,0(4)
C2-C3	137,0(6)	140,6(5)	138,8(5)
C3-C4	138,4(6)	137,7(6)	137,3(5)
C4-C5	138,7(5)	138,7(5)	141,1(4)
C5-C6	150,1(5)	152,0(4)	141,2(4)
C6-N2	148,8(5)	142,7(4)	133,7(4)
N2-C7	150,9(5)	141,9(4)	134,0(4)
C7-C8	147,6(5)	149,8(4)	141,1(4)
C8-C9	140,0(6)	139,6(4)	139,3(4)
C9-C10	137,2(6)	137,2(4)	137,0(4)
C10-C11	138,5(6)	140,2(4)	139,6(4)
C11-C12	139,4(6)	137,5(4)	138,2(4)
C12-N3	135,6(5)	135,0(4)	133,9(4)
C8-N3	133,4(5)	134,8(3)	138,4(3)
Fe-N1	198,7(3)	220,6(2)	196,9(2)
Fe-N2	203,1(3)	200,6(2)	190,5(2)
Fe-N3	198,7(3)	222,2(2)	196,9(2)
N1-Fe-N2	83,6(1)	75,81(9)	82,1(0)
N2-Fe-N3	83,2(1)	75,36(9)	82,4(1)
N1-Fe-N3	86,7(1)	151,17(8)	164,4(1)

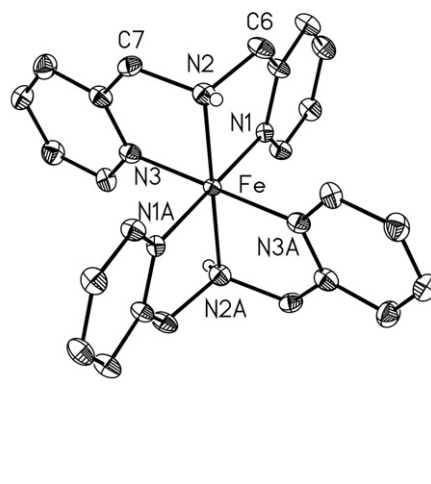


**Fig. 3.** Molecular structure and numbering scheme of the cation [Fe{HN(CH<sub>2</sub>Py)<sub>2</sub>}<sub>2</sub>]<sup>2+</sup> of **1**. The ellipsoids represent a probability of 40%, for clarity reasons only the amine H atoms are drawn.

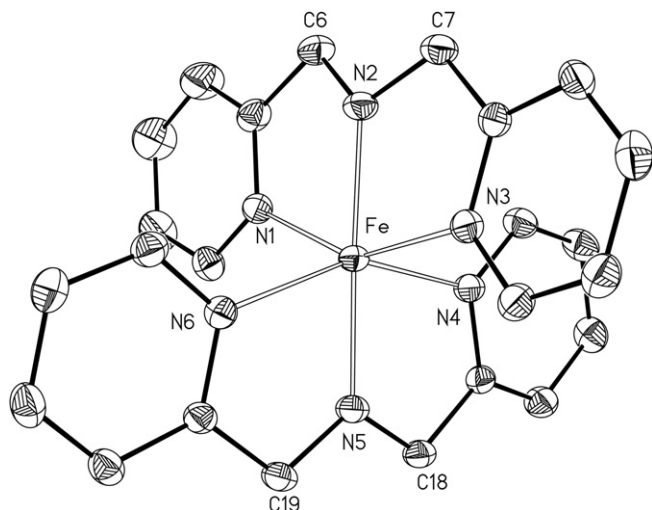


**Fig. 4.** Molecular structure and numbering scheme of  $[\text{Fe}(\text{N}(\text{CH}_2\text{Py})_2)_2]_2$  (**4**). The ellipsoids represent a probability of 40%, H atoms are neglected for the sake of clarity.

Molecular structures and numbering schemes of the iron derivatives **2b** and **3** are shown in the Figs. 5 and 6. The molecular structures of **2a** and **2c** are very similar to **2b**. The M–N2 bonds (av. values for **2a**: 220.8, **2b**: 214.9, **2c**: 212.2, and **3**: 211.5 pm) strongly reflect the radii of the metal cations  $\text{M}^{2+}$  (radius of high spin/low spin  $\text{Mn}^{2+}$  0.97/0.81 and  $\text{Fe}^{2+}$  0.92/0.75, as well as of  $\text{Zn}^{2+}$  0.88 pm). Due to the bridging position of the amido group the M–N2 bond lengths are larger as observed in the mononuclear derivatives discussed before. The Fe– $\text{N}_{\text{Py}}$  distances resemble similar trends but are larger than the other M–N2 bond lengths. The rather large Zn–N1/3 distances could also be discussed on the basis of an N1–Zn–N3 4-electron 3-center bond with the amido bases binding into the  $p_z(\text{Zn})$  orbital. Manganese often favors high spin states and shows peculiar properties resembling similarities with the magnesium compounds [32].

### 3. Summary and conclusion

Di(2-pyridylmethyl)amine enriches the possible reaction spectrum in comparison to the 2-pyridylmethylamines. In Scheme 3 the reactivity of this amine is shown. The combination of redox and

**Table 3**

Selected structural parameters for the compounds  $[\text{R}-\text{M}\{\mu\text{-N}(\text{CH}_2\text{Py})_2\}_2]$  of manganese (**2a**), iron (**2b** and **3**), and zinc (**2c**). The radii are given for hexa-coordinate metal ions, the first value refers to low spin state, the second to high spin state metal ions (bond lengths [pm] and angles [°]).

Position	<b>2a</b>	<b>2b</b>	<b>2c</b>	<b>3</b>
M	Mn	Fe	Zn	Fe
$r(\text{M}^{2+})$	0.81/0.97	0.69/0.785	0.88	0.69/0.785
R	$\text{N}(\text{SiMe}_3)_2$	$\text{N}(\text{SiMe}_3)_2$	$\text{N}(\text{SiMe}_3)_2$	$\text{C}_6\text{H}_2\text{-2,4,6-Me}_3$
M–N1	229.3(2)	222.5(2)	227.3(2)	221.2(3)
M–N2	223.0(2)	213.5(2)	215.3(2)	212.2(3)
M–N3	226.3(2)	219.1(2)	221.6(2)	219.2(3)
M–N4/C13	211.3(2)	205.0(2)	201.8(2)	212.6(4)
M–N2A	218.5(2)	216.2(2)	209.1(2)	210.7(3)
N2–C7	147.0(3)	145.9(3)	146.1(2)	146.1(5)
N2–C6	145.9(3)	146.0(3)	146.0(2)	146.0(5)
Si1–N4	169.4(2)	170.4(2)	170.3(2)	–
Si2–N2	170.0(2)	170.3(2)	170.0(2)	–
M–M(A)	304.26(7)	297.02(6)	297.17(4)	283.4(1)
N2–M–N2A	91.71(7)	91.44(7)	90.24(6)	95.9(1)
N4–M–N2A	122.66(7)	117.95(7)	122.40(6)	125.4(1)
N4–M–N2	145.49(8)	150.49(7)	147.30(6)	–
N3–M–N1	141.45(7)	147.58(7)	144.33(6)	147.2(1)
M–N2–MA	87.14(7)	87.47(7)	88.87(6)	84.1(1)

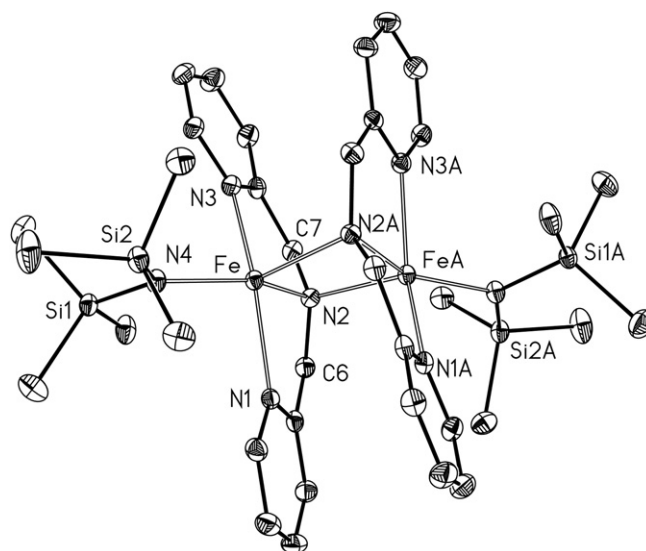


**Fig. 5.** Molecular structure and numbering scheme of  $[(\text{Me}_3\text{Si})\text{N}-\text{Fe}(\mu\text{-N}(\text{CH}_2\text{Py})_2)_2]_2$  (**2b**). The ellipsoids represent a probability of 40%, the hydrogen atoms are neglected for clarity reasons. The Mn (**2a**) and Zn derivatives (**2c**) show very similar molecular structures.

deprotonation steps starting from the amide ( $\text{H}_2\text{L}^-$ ) leads to a 1,3-di(2-pyridyl)-2-azaallyl ligand ( $\text{L}^{\text{ox}2-}$ ) which resembles the dehydrogenated 1,3-di(2-pyridylmethyl)amide anion. Iron(II), cobalt(II) and zinc(II) bis[bis(trimethylsilyl)amides] are able to follow this reaction sequence whereas the reaction of  $\text{Mn}[\text{N}(\text{SiMe}_3)_2]_2$  with  $\text{HN}(\text{CH}_2\text{Py})_2$  only gives the heteroleptic dinuclear complex  $[(\text{Me}_3\text{Si})_2\text{N}-\text{Mn}\{\mu\text{-N}(\text{CH}_2\text{Py})_2\}_2]_2$  and the formation of an azaallyl ligand does not occur under these reaction conditions. This finding is in agreement with the observations that manganese(II) with a high spin state is rather similar to magnesium(II) in many aspects (ionic compounds, weak redox activity) but that iron(II), cobalt(II) and zinc(II) are highly redox active and able to activate C–H bonds.

The reaction behaviour of  $[\text{M}\{\text{N}(\text{SiMe}_3)_2\}_2]_2$  toward di(2-pyridylmethyl)amine in dependency of the 3d-metal (and hence the valence electron count) can be summarized as follows:

- The iron(II) derivatives are the most stable compounds allowing the isolation of complexes of the types  $[\text{Fe}\{\text{HN}(\text{CH}_2\text{Py})_2\}_2]^{2+}$  (**1** with amino ligands),  $[(\text{Me}_3\text{Si})_2\text{N}-\text{Fe}\{\mu\text{-N}(\text{CH}_2\text{Py})_2\}_2]$  (**2b**),  $[\text{Mes}-\text{Fe}-\text{N}(\text{CH}_2\text{Py})_2]$  (**3**), and  $[\text{Fe}\{\text{N}(\text{CH}_2\text{Py})_2\}_2]$  (**4**, containing amido ligands), as well as  $[\text{Fe}\{\text{N}(\text{CHPy})_2\}_2]$  (**5a** with 2-azaallyl ligands). Similar derivatives are also known for zinc(II). The amido ligands undergo a transformation to the 2-azaallylic systems already at room temperature (dehydrogenation).
- The transamination of  $\text{HN}(\text{CH}_2\text{Py})_2$  with  $[\text{Mn}\{\text{N}(\text{SiMe}_3)_2\}_2]_2$  leads to the formation of  $[(\text{Me}_3\text{Si})_2\text{N}-\text{Mn}\{\mu\text{-N}(\text{CH}_2\text{Py})_2\}_2]$  (**2a**). This complex is stable at room temperature.
- The reaction of  $[\text{Co}\{\text{N}(\text{SiMe}_3)_2\}_2]_2$  with  $\text{HN}(\text{CH}_2\text{Py})_2$  yields  $[\text{Co}\{\text{N}(\text{CHPy})_2\}_2]$  (**5b**) with 2-azaallyl ligands regardless of the applied stoichiometry. Di(2-pyridylmethyl)amido ligands seem to be unstable in the vicinity of cobalt(II).
- The degradation of di(2-pyridylmethyl)amides and formation of 1,3-di(2-pyridyl)-2-azaallyl anions proceeds via the intermediate radical  $[(2\text{-Py-CH})_2\text{N}\cdot]$ .

The di(2-pyridylmethyl)amido complex of iron(II) is not obtainable via a metathetical approach (reaction of  $\text{LiN}(\text{CH}_2\text{Py})_2$  with  $\text{FeCl}_2$ ) because lithium di(2-pyridylmethyl)amide, a rather strong deprotonation reagent, immediately lithiates the methylene

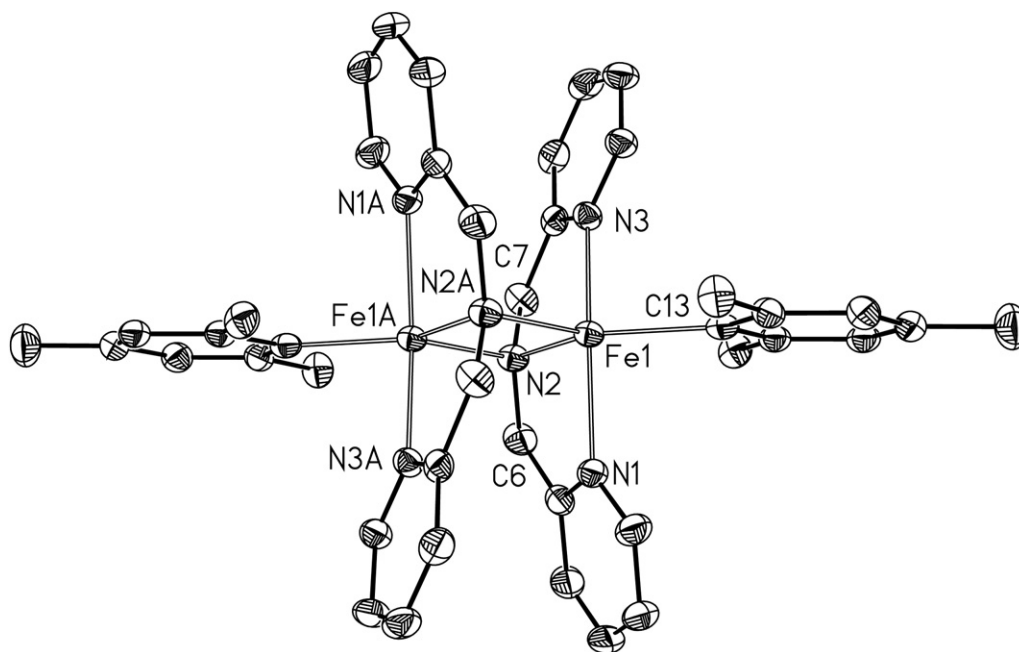


**Fig. 6.** Molecular structure and numbering scheme of  $[\text{Mes-Fe}\{\mu\text{-N}(\text{CH}_2\text{Py})_2\}_2]_2$  (**3**). The ellipsoids represent a probability of 40%, hydrogen atoms are not shown for clarity reasons.

fragments. In contrast to this finding, the compound  $[\text{Fe}\{\text{N}(\text{CHPy})_2\}_2]$  with 1,3-di(2-pyridyl)-2-azaallyl ligands can be isolated from such procedure.

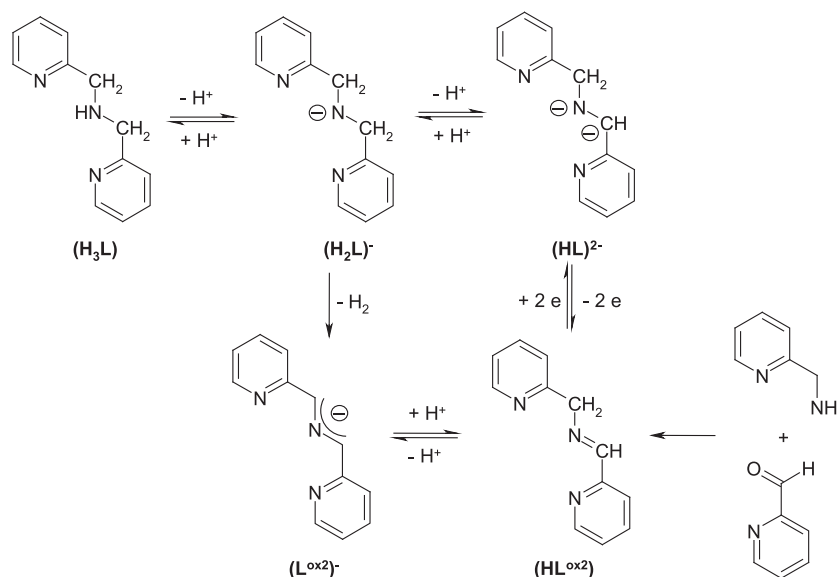
Activation of C-H bonds was investigated by using 3d transition metal complexes of manganese, iron, cobalt and iron. Depending on the metal dehydrogenation can be achieved converting di(2-pyridylmethyl)amides into di(2-pyridyl)-2-azaallyl anions. These results extend the spectrum of 3d metals in C-H bond activation which can be used for C–C bond formation [33].

## 4. Experimental details

### 4.1. General procedure

All manipulations were carried out in an argon atmosphere under anaerobic conditions. The compounds are moisture and air

sensitive. Prior to use, all solvents were thoroughly dried and distilled in an argon atmosphere. Starting  $[\text{M}\{\text{N}(\text{SiMe}_3)_2\}_2]_2$  of manganese [18], iron [19], cobalt [22], and zinc [30] as well as dimesityl iron [31] were prepared according to literature procedures. Azaallyl complexes of the type  $\text{M}\{\text{N}(\text{CHPy})_2\}_2$  for Fe (**5a**) and Co (**5b**) were also prepared previously by another route via deprotonation of  $\text{PyCH}_2\text{-N}=\text{CHPy}$  with  $[\text{M}\{\text{N}(\text{SiMe}_3)_2\}_2]_2$  or metathetical by addition of  $\text{LiN}(\text{CHPy})_2$  to  $(\text{thf})_2\text{FeBr}_2$  or  $\text{CoCl}_2$  [26]. The synthesis of  $\text{Zn}\{\text{N}(\text{CHPy})_2\}_2$  (**5c**) was already reported earlier [27], but a reinvestigation was performed in order to shed light on the reaction mechanism. IR spectra were recorded at Nujol solutions between KBr windows. The magnetic properties were determined by a Gouy magnetic balance at 290 K and SQUID measurements. These compounds are sensitive towards moisture and air. In addition, weighing and handling of these substances for C,H,N analytical data proved to be challenging.



**Scheme 3.** Schematic representation of the reaction spectrum of di(2-pyridylmethyl)amine.

#### 4.1.1. Synthesis of $[\text{Fe}(\text{HN}(\text{CH}_2\text{Pyr})_2)_2]\text{Cl}_2 \cdot \text{CH}_2\text{Cl}_2$ (**1**)

Di(2-pyridylmethyl)amine (0.37 g, 1.89 mmol) was dissolved in 10 mL of THF at  $-78^\circ\text{C}$ . Then 1.2 mL of a 1.6 M solution of *n*-BuLi in hexane (1.92 mmol) was dropped into this solution. Afterwards this solution was added at  $-78^\circ\text{C}$  to a suspension of 0.24 g of  $\text{FeCl}_2$  (1.89 mmol) in 10 mL of THF. Thereafter the reaction mixture was warmed to r.t. and a red solid precipitated from this blue solution. This red solid was collected and dried in vacuo. Recrystallization from  $\text{CH}_2\text{Cl}_2$  afforded 0.45 g of crystalline **1** (Yield: 0.86 mmol, 93%). M.p.:  $223^\circ\text{C}$ . IR ( $\text{cm}^{-1}$ ):  $\tilde{\nu} = 3400$  w br, 3109 m, 3084 m, 2724 w, 1607 m, 1570 w, 1513 w, 1484 s, 1312 m, 1283 m, 1153 w, 1133 m, 1109 w, 1076 w, 1064 w, 1021 w, 973 w, 945 w, 912 m, 892 w, 820 w, 773 s, 724 vs, 691 m, 649 w, 524 w. MS (DEI):  $m/z = 291$  ( $[\text{FeClHN}(\text{CH}_2\text{-Pyr})_2]^+$ , <3%), 200 ( $[\text{HN}(\text{CH}_2\text{-Pyr})_2 + \text{H}]^+$ , 66%), 107 ( $[\text{Pyr-CH}_2\text{-NH}]^+$ , 95%), 93 ( $[\text{Pyr-CH}_3]^+$ , 100%). Elemental analysis ( $\text{C}_{25}\text{H}_{28}\text{Cl}_4\text{Fe-N}_6$ , 610.19): calc.: C 49.06, H 4.61, N 13.73; found: C 46.42, H 4.34, N 12.37.

#### 4.1.2. Synthesis of $[(\text{Me}_3\text{Si})\text{N-Mn-N}(\text{CH}_2\text{Pyr})_2]_2$ (**2a**)

A solution of 0.34 g of  $[\text{Mn}(\text{N}(\text{SiMe}_3)_2)_2]$  (0.45 mmol) in 5 mL of diethyl ether was cooled to  $-78^\circ\text{C}$ . A second solution of 0.37 g of di(2-pyridylmethyl)amine (1.80 mmol) in 3 mL of diethyl ether was layered on top of this solution. This mixture was kept at  $-18^\circ\text{C}$  for 2 days. Yellow crystals of **2a** (0.25 g, 0.31 mmol; 67%) formed, were washed several times with cold diethyl ether and then dried under vacuum. M.p.:  $143^\circ\text{C}$ . IR ( $\text{cm}^{-1}$ ):  $\tilde{\nu} = 1602$  s, 1571 m, 1479 m, 1435 s, 1342 m, 1278 m, 1245 s, 1233 s, 1150 m, 1131 m, 1097 m, 1048 m, 1033 m, 997 vs br, 879 vs, 830 vs br, 773 m, 729 m, 659 m, 638 m, 605 m. MS (DEI):  $m/z = 447$  ( $[\text{Mn}(\text{N}(\text{CH}_2\text{-Pyr})_2)_2]^+$ , 1%), 414 ( $[\text{MnN}(\text{CH}_2\text{Pyr})_2\text{N}(\text{SiMe}_3)_2]^+$ , <1%), 161 ( $[\text{HN}(\text{SiMe}_3)_2]^+$ , 6%), 146 ( $[\text{HN}(\text{SiMe}_3)_2 - \text{Me}]^+$ , 90%), 93 ( $[\text{Pyr-CH}_3]^+$ , 100%). Magnetism:  $\mu_{\text{eff}} = 6.5 \mu_{\text{B}}$ , 300 K.

#### 4.1.3. Synthesis of $[(\text{Me}_3\text{Si})\text{N-Fe-N}(\text{CH}_2\text{Pyr})_2]_2$ (**2b**)

A solution of 0.29 g of  $[\text{Fe}(\text{N}(\text{SiMe}_3)_2)_2]$  (0.39 mmol) in 12 mL of diethyl ether was layered at r.t. with a solution of 0.15 g of di(2-pyridylmethyl)amine (0.78 mmol) in 5 mL of diethyl ether. Within 1 day 0.15 g of pink needle-shaped crystals of **2b** (0.18 mmol, 47%) precipitated which were dried under reduced pressure. M.p.:  $180^\circ\text{C}$ . IR ( $\text{cm}^{-1}$ ):  $\tilde{\nu} = 1600$  m, 1570 w, 1435 m, 1339 w, 1276 m, 1247 m, 1236 s, 1150 m, 1134 m, 1098 w, 1048 w, 1032 m, 974 vs, 875 s, 830 s, 778 m, 750 s, 727 m, 658 m, 608 w. MS (DEI):  $m/z = 448$  ( $[\text{Fe}(\text{N}(\text{CH}_2\text{-Pyr})_2)_2]^+$ , 11%), 414 ( $[\text{Fe-N}(\text{CH}_2\text{Pyr})_2\text{N}(\text{SiMe}_3)_2]^+$ , 10%), 161 ( $[\text{HN}(\text{SiMe}_3)_2]^+$ , 7%), 146 ( $[\text{HN}(\text{SiMe}_3)_2 - \text{Me}]^+$ , 100%). Elemental analysis ( $\text{C}_{36}\text{H}_{60}\text{Fe}_2\text{N}_8\text{Si}_4$ , 828.95): calc.: C 52.16, H 7.30, N 13.52; found: C 51.82, H 6.91, N 13.46. Magnetism:  $\mu_{\text{eff}} = 7.5 \mu_{\text{B}}$ , 300 K.

#### 4.1.4. Synthesis of $[(\text{Me}_3\text{Si})\text{N-Zn-N}(\text{CH}_2\text{Pyr})_2]_2$ (**2c**)

A solution of 0.25 g of di(2-pyridylmethyl)amine (1.34 mmol) in 2 mL of diethyl ether was layered at r.t. on top of a solution of 0.48 g of  $\text{Zn}[\text{N}(\text{SiMe}_3)_2]_2$  (1.24 mmol) in 4 mL of diethyl ether. Within 24 h 0.40 g of colorless rod-like crystals of **2c** (0.48 mmol, 77%) precipitated and were collected and dried under vacuum.  $^1\text{H-NMR}$  ( $[\text{D}_8]$  THF, 200 MHz, 253 K):  $\delta = 8.40$  (d br,  $^3\text{J}(\text{H}_1, \text{H}_2) = 5.0$  Hz, 1 H, H1), 7.43 (dt,  $^3\text{J}(\text{H}_3, \text{H}_2/4) = 7.6$  Hz,  $^4\text{J}(\text{H}_3, \text{H}_1) = 1.6$  Hz, 1 H, H3), 6.95 (t br,  $^3\text{J}(\text{H}_2, \text{H}_1/3) = 6.3$  Hz, 1 H, H2), 6.86 (d br,  $^3\text{J}(\text{H}_4, \text{H}_3) = 7.8$  Hz, 1 H, H4), 0.04 (s, 9 H, Si(CH<sub>3</sub>)<sub>3</sub>). IR ( $\text{cm}^{-1}$ ):  $\tilde{\nu} = 2732$  m, 2672 w, 1602 s, 1575 m, 1480 m, 1435 s, 1342 m, 1278 m, 1247 s, 1235 s, 1149 m, 1139 m, 1099 m, 1048 m, 1038 m, 1011 m, 985 vs, 881 s, 830 vs, 780 m, 752 s, 729 m, 659 m, 636 m, 609 m, 496 m. MS (DEI):  $m/z = 456$  ( $[\text{Zn}(\text{N}(\text{CH}_2\text{-Pyr})_2)_2]^+$ , 3%), 161 ( $[\text{HN}(\text{SiMe}_3)_2]^+$ , 7%), 146 ( $[\text{HN}(\text{SiMe}_3)_2 - \text{Me}]^+$ , 45%). Elemental analysis ( $\text{C}_{36}\text{H}_{60}\text{N}_6\text{Si}_4\text{Zn}_2$ , 848.08): calc.: C 50.98, H 7.13, N 13.21; found: C 50.39, H 7.05, N 13.32.

#### 4.1.5. Synthesis of $[\text{Mes-Fe-N}(\text{CH}_2\text{Pyr})_2]_2$ (**3**)

At  $-20^\circ\text{C}$  a solution of 0.28 g of dimesityl iron (0.94 mmol) in 10 mL of toluene was layered with a solution of 0.19 g of di(2-pyridylmethyl)amine (0.94 mmol) in 13 mL of toluene and kept at  $-20^\circ\text{C}$  for several days. Black crystals formed within 3 days which were collected, washed with a small amount of cold toluene and dried in vacuo. Yield: 0.24 g (0.30 mmol, 69%). M.p.:  $288^\circ\text{C}$ . IR ( $\text{cm}^{-1}$ ):  $\tilde{\nu} = 2789$  m, 2725 w, 1597 m, 1567 m, 1478 s, 1456 vs, 1435 vs, 1337 m, 1274 m, 1210 w, 1151 m, 1127 m, 1097 m, 1067 m, 1046 m, 1029 m, 1009 m, 981 w, 909 w, 848 m, 763 m, 751 s, 726 m, 648 w, 642 w, 636 w, 629 w, 536 w, 485 w. MS (DEI):  $m/z = 448$  ( $[\text{Fe}(\text{N}(\text{CH}_2\text{-Pyr})_2)_2]^+$ , 5%), 200 ( $[\text{HN}(\text{CH}_2\text{-Pyr})_2 + \text{H}]^+$ , 82%), 120 ( $[\text{Mes} + \text{H}]^+$ , 93%), 105 ( $[\text{Mes} - \text{Me}]^+$ , 93%), 93 ( $[\text{Pyr-CH}_3]^+$ , 100%). Elemental analysis ( $\text{C}_{42}\text{H}_{46}\text{Fe}_2\text{N}_6$ , 764.55): calc.: C 67.57, H 6.21, N 11.26; found: C 64.12, H 6.21, N 11.55. Magnetism:  $\mu_{\text{eff}} = 8.0 \mu_{\text{B}}$ , 300 K.

#### 4.1.6. Synthesis of $[\text{Fe}[\text{N}(\text{CH}_2\text{Pyr})_2]_2]$ (**4**)

A solution of 0.21 g of  $[\text{Fe}[\text{N}(\text{SiMe}_3)_2]_2]$  (0.28 mmol) in 2 mL of THF was cooled to  $-78^\circ\text{C}$ . At this temperature a solution of 0.22 g of di(2-pyridylmethyl)amine (1.12 mmol) in 5 mL of diethyl ether was added dropwise. Then the reaction mixture was filtered at  $-30^\circ\text{C}$ . The blue mother liquor was kept at or below  $-20^\circ\text{C}$ . Within a few days, 0.12 g of long needle-like colorless crystals of **4** (0.26 mmol, 40%) precipitated. These crystals contain thf and Et<sub>2</sub>O. At r.t. these ethers are liberated and the remaining compound dissolves in these ethers. Therefore, no m.p. can be given. IR ( $\text{cm}^{-1}$ ):  $\tilde{\nu} = 1590$  s, 1569 m, 1429 s, 1175 w, 1133 m, 1047 m, 994 m, 753 s, 626 w. MS (DEI):  $m/z = 448$  ( $[\text{Fe}(\text{N}(\text{CH}_2\text{-Pyr})_2)_2]^+$ , 2%), 200 ( $[\text{HN}(\text{CH}_2\text{-Pyr})_2 + \text{H}]^+$ , 82%), 107 ( $[\text{Pyr-CH}_2\text{-NH}]^+$ , 55%), 93 ( $[\text{Pyr-CH}_3]^+$ , 100%).

#### 4.1.7. Synthesis of $[\text{Fe}[\text{N}(\text{CHPy})_2]_2]$ (**5a**)

A solution of 0.44 g of  $[\text{Fe}[\text{N}(\text{SiMe}_3)_2]_2]$  (0.59 mmol) in 5 mL of THF was added dropwise at  $-78^\circ\text{C}$  to a stirred solution of 0.24 g of di(2-pyridylmethyl)amine (1.19 mmol) in 5 mL of diethyl ether. Then the reaction mixture was warmed to r.t. and stirred for additional 30 min. After filtration the volume of the mother liquor was reduced to half of the original amount. Within several days at r.t. 0.14 g of colorless platelets of **5a** (0.31 mmol, 52%) precipitated which were dried under vacuum. M.p.:  $335^\circ\text{C}$ . IR ( $\text{cm}^{-1}$ ):  $\tilde{\nu} = 1585$ , 1542 m br, 1382 vs br, 1320 m, 1285 m, 1261 m, 1176 s, 1132 vs, 1022 m, 1005 s, 844 w, 757 m, 732 m, 684 m, 537 w, 517 w, 479 w. MS (DEI):  $m/z = 448$  ( $[\text{M}]^+$ , 63%), 252 ( $[\text{Fe-N}(\text{CH}_2\text{-Pyr})_2]^+$ , 45%), 107 ( $[\text{Pyr-CH}_2\text{-NH}]^+$ , 45%), 93 ( $[\text{Pyr-CH}_3]^+$ , 100%). Elemental analysis ( $\text{C}_{24}\text{H}_{20}\text{Fe-N}_6$ , 448.30): calc.: C 64.30, H 4.50, N 18.75; found: C 63.40, H 4.62, N 18.54.

#### 4.1.8. Synthesis of $[\text{Co}[\text{N}(\text{CHPy})_2]_2]$ (**5b**)

A solution of 0.63 g of di(2-pyridylmethyl)amine (3.16 mmol) in 3 mL of diethyl ether was layered at  $-78^\circ\text{C}$  on top of a solution of 0.60 g of  $[\text{Co}[\text{N}(\text{SiMe}_3)_2]_2]$  (0.79 mmol) in 5 mL of diethyl ether. Within 2 days at this temperature 0.34 g of dark violet platelets of **5b** (0.76 mmol, 48%) precipitated and were collected and dried under vacuum. M.p.:  $276^\circ\text{C}$ . IR ( $\text{cm}^{-1}$ ):  $\tilde{\nu} = 1546$  m, 1459 m, 1395 vs br, 1320 m, 1286 m, 1193 s, 1135 vs, 1071 w, 1045 w, 986 s, 788 w, 753 m, 731 m, 670 w, 515 w. MS (DEI):  $m/z = 451$  ( $[\text{M}]^+$ , 49%), 255 ( $[\text{CoN}(\text{CH}_2\text{-Pyr})_2]^+$ , 28%), 107 ( $[\text{Pyr-CH}_2\text{-NH}]^+$ , 58%), 93 ( $[\text{Pyr-CH}_3]^+$ , 100%). Elemental analysis ( $\text{C}_{24}\text{H}_{20}\text{CoN}_6$ , 451.39): calc.: C 63.86, H 4.43, N 18.63; found: C 63.00, H 4.96, N 17.58. Magnetism:  $\mu_{\text{eff}} = 3.8 \mu_{\text{B}}$ , 300 K.

#### 4.1.9. Synthesis of $[\text{Zn}[\text{N}(\text{CHPy})_2]_2]$ (**5c**)

M.p.  $133^\circ\text{C}$ .  $^1\text{H-NMR}$  ( $[\text{D}_8]$  THF, 200 MHz, 253 K):  $\delta = 8.40$  (d br,  $^3\text{J}(\text{H}_1, \text{H}_2) = 5.0$  Hz, 1 H, H1), 7.43 (dt,  $^3\text{J}(\text{H}_3, \text{H}_2/4) = 7.6$  Hz,  $^4\text{J}(\text{H}_3,$

**Table 4**  
Crystal data and refinement details for the X-ray structure determinations of **1**, **2a–2c**, **3**, and **4**.

Compound	<b>1</b>	<b>2a</b>	<b>2a-thf</b>	<b>2a-ether</b>	<b>2b</b>	<b>2c</b>	<b>3</b>	<b>4</b>
formula	[C <sub>24</sub> H <sub>26</sub> Fe-N <sub>6</sub> ] <sup>2+</sup> 2(Cl <sup>-</sup> ), 2(CH <sub>2</sub> Cl <sub>2</sub> )	C <sub>36</sub> H <sub>60</sub> Mn <sub>2</sub> N <sub>8</sub> Si <sub>4</sub>	C <sub>36</sub> H <sub>60</sub> Mn <sub>2</sub> N <sub>8</sub> Si <sub>4</sub> 0.25(C <sub>4</sub> H <sub>8</sub> O)	C <sub>36</sub> H <sub>60</sub> Mn <sub>2</sub> N <sub>8</sub> Si <sub>4</sub> 2(C <sub>4</sub> H <sub>10</sub> O)	C <sub>36</sub> H <sub>60</sub> Fe <sub>2</sub> N <sub>8</sub> Si <sub>4</sub> 2(C <sub>4</sub> H <sub>10</sub> O)	C <sub>36</sub> H <sub>60</sub> N <sub>8</sub> Si <sub>4</sub> Zn <sub>2</sub> 2(C <sub>4</sub> H <sub>10</sub> O)	C <sub>42</sub> H <sub>46</sub> Fe <sub>2</sub> N <sub>6</sub> 2(C <sub>7</sub> H <sub>8</sub> )	C <sub>24</sub> H <sub>24</sub> Fe-N <sub>6</sub> C <sub>4</sub> H <sub>8</sub> O, 0.25(C <sub>4</sub> H <sub>10</sub> O)
fw (g mol <sup>-1</sup> )	695.11	827.16	845.19	975.40	977.22	996.26	930.82	542.98
T/ <sup>o</sup> C	-90(2)	-90(2)	-90(2)	-90(2)	-90(2)	-90(2)	-90(2)	-90(2)
crystal system	monoclinic	orthorhombic	triclinic	monoclinic	monoclinic	monoclinic	monoclinic	monoclinic
space group	P 2 <sub>1</sub> /n	P ca2 <sub>1</sub>	P $\bar{1}$	C 2/c	C 2/c	C 2/c	P 2 <sub>1</sub> /c	C 2/c
a/Å	9.4237(9)	16.9586(4)	11.2174(7)	15.1506(6)	14.9801(4)	14.9743(5)	12.0971(4)	30.2251(9)
b/Å	14.2953(9)	11.4369(2)	11.7465(4)	19.5335(5)	19.5413(9)	19.5528(4)	16.2760(7)	8.8782(3)
c/Å	11.4918(6)	22.8730(5)	17.7512(9)	18.3900(8)	18.3671(7)	18.3648(6)	14.8301(6)	21.7397(5)
$\alpha$ / <sup>o</sup>	90	90	90.013(3)	90	90	90	90	90
$\beta$ / <sup>o</sup>	94.186(5)	90	98.807(2)	96.497(2)	96.335(2)	96.619(1)	111.581(2)	104.50(2)
$\gamma$ / <sup>o</sup>	90	90	94.995(3)	90	90	90	90	90
V/Å <sup>3</sup>	1543.98(19)	4436.30(16)	2302.4(2)	5407.5(3)	5343.8(3)	5341.2(3)	2715.24(18)	5647.8(3)
Z	2	4	2	4	4	4	2	8
$\rho$ (g·cm <sup>-3</sup> )	1.495	1.238	1.219	1.198	1.215	1.239	1.139	1.277
$\mu$ (cm <sup>-1</sup> )	10.35	7.11	6.87	5.96	6.74	10.29	5.73	5.67
measured data	10 594	30 224	16 731	19 209	18 112	18 677	17 679	18 457
data with I > 2 $\sigma$ (I)	2325	7701	5453	4053	4248	4726	4549	4765
unique data/R <sub>int</sub>	3526/0.0627	9316/0.0603	10 469/0.0657	6183/0.0663	6114/0.0596	6110/0.0446	6137/0.0532	6433/0.0397
wR <sub>2</sub> (all data, on F <sup>2</sup> ) <sup>a</sup>	0.1656	0.0794	0.1822	0.1111	0.1019	0.0828	0.2334	0.1769
R <sub>1</sub> (I > 2 $\sigma$ (I)) <sup>a</sup>	0.0571	0.0366	0.0660	0.0428	0.0421	0.0330	0.0671	0.0536
s <sup>b</sup>	1.028	1.001	1.017	1.015	1.010	1.015	1.103	1.027
Res. dens./e·Å <sup>-3</sup>	1.046/-0.562	0.382/-0.292	0.920/-0.433	0.289/-0.397	0.314/-0.450	0.372/-0.527	1.134/-0.552	1.330/-0.451
CCDC No.	763 994	770 773	763 995	763 996	763 997	763 998	763 999	763 900

wR<sub>2</sub> =  $\{\sum[w(F_o^2 - F_c^2)]^2 / \sum[w(F_o^2)]\}^{1/2}$  with  $w^{-1} = \sigma^2(F_o^2) + (aP)^2 + bP$ ;  $P = [2F_c^2 + \text{Max}(F_o^2)]/3$ .

<sup>a</sup> Definition of the R indices:  $R_1 = (\sum|F_o| - |F_c|) / \sum|F_o|$ .

<sup>b</sup>  $s = \{\sum[w(F_o^2 - F_c^2)]^2 / (N_o - N_p)\}^{1/2}$ .

H1) = 1,6 Hz, 1 H, H3), 6,95 (t br, <sup>3</sup>J(H2,H1/3) = 6,3 Hz, 1 H, H2), 6,86 (d br, <sup>3</sup>J(H4,H3) = 7,8 Hz, 1 H, H4), 0,04 (s, 9 H, Si(CH<sub>3</sub>)<sub>3</sub>). IR (cm<sup>-1</sup>):  $\bar{\nu} = 2732$  m, 2672 w, 1602 s, 1575 m, 1480 m, 1435 s, 1342 m, 1278 m, 1247 s, 1235 s, 1149 m, 1139 m, 1099 m, 1048 m, 1038 m, 1011 m, 985 vs, 881 s, 830 vs, 780 m, 752 s, 729 m, 659 m, 636 m, 609 m, 496 m. MS (DEI): *m/z* = 456 ([Zn(N(CH<sub>2</sub>-Pyr)<sub>2</sub>)<sub>2</sub>]<sup>+</sup>, 3%), 161 ([HN(SiMe<sub>3</sub>)<sub>2</sub>]<sup>+</sup>, 7%), 146 ([HN(SiMe<sub>3</sub>)<sub>2</sub> - Me]<sup>+</sup>, 45%). Elemental analysis (C<sub>36</sub>H<sub>60</sub>N<sub>6</sub>Si<sub>4</sub>Zn<sub>2</sub>, 848.08): calc.: C 50.98, H 7.13, N 13.21; found: C 50.39, H 7.05, N 13.32.

#### 4.1.10. X-ray structure determinations

The intensity data for the compounds were collected on a Nonius KappaCCD diffractometer using graphite-monochromated Mo-K $\alpha$  radiation. Data were corrected for Lorentz and polarization effects but not for absorption effects [34,35]. Crystal data and refinement details for the X-ray structure determinations are summarized in Table 4.

The structures were solved by direct methods (SHELXS) [36] and refined by full-matrix least squares techniques against F<sub>o</sub><sup>2</sup> (SHELXL-97) [37]. All hydrogen atoms were included at calculated positions with fixed thermal parameters. All non-disordered, non-hydrogen atoms were refined anisotropically [37]. XP (SIEMENS Analytical X-ray Instruments, Inc.) was used for structure representations.

#### Acknowledgements

These results were presented on the International Conference on Coordination Chemistry in July 2008 in Jerusalem, Israel (ICCC38) and A. Malassa thanks the Deutsche Forschungsgemeinschaft (DFG, Bonn-Bad Godesberg, Germany) for a generous stipend to cover the travel expenses. We also appreciate the financial support of the Deutsche Forschungsgemeinschaft (DFG, Bonn-Bad Godesberg, Germany). A. Malassa is also grateful to the Carl-Zeiss-Stiftung (Stuttgart, Germany) for a generous Ph.D. grant.

#### References

- [1] M. Westerhausen, A.N. Kneifel, N. Makropoulos, Inorg. Chem. Commun. 7 (2004) 990–993.
- [2] M. Westerhausen, T. Bollwein, N. Makropoulos, S. Schneiderbauer, M. Suter, H. Nöth, P. Mayer, H. Piotrowski, K. Polborn, A. Pfizner, Eur. J. Inorg. Chem. (2002) 389–404.
- [3] J.T.B.H. Jastrzebski, J.M. Klerks, G. van Koten, K. Vrieze, J. Organomet. Chem. 210 (1981) C49–C53.
- [4] G. van Koten, J.T.B.H. Jastrzebski, K. Vrieze, J. Organomet. Chem. 250 (1983) 49–61.
- [5] A.L. Spek, J.T.B.H. Jastrzebski, G. van Koten, Acta Cryst. C43 (1987) 2006–2007.
- [6] E. Wissing, S. van der Linden, E. Rijnberg, J. Boersma, W.J.J. Smeets, A.L. Spek, G. van Koten, Organometallics 13 (1994) 2602–2608.
- [7] M. Westerhausen, T. Bollwein, N. Makropoulos, T.M. Rotter, T. Habereeder, M. Suter, H. Nöth, Eur. J. Inorg. Chem. (2001) 851–857.
- [8] A. Malassa, N. Herzer, H. Görls, M. Westerhausen, Ph.D. thesis, Jena/Germany, 2010.
- [9] N.Y. Murakami Iha, M.A. de Almeida Azzellini, S. Utsuno, Polyhedron 17 (1998) 3379–3390.
- [10] K. Ogura, Y. Kurasawa, Y. Yamaguchi, Y. Okamoto, Heterocycles 59 (2003) 283–291.
- [11] M. Westerhausen, T. Bollwein, P. Mayer, H. Piotrowski, Z. Anorg. Allg. Chem. 628 (2002) 1425–1432.
- [12] C.C. Lu, E. Bill, T. Weyhermüller, E. Bothe, K. Wiegardt, J. Am. Chem. Soc. 130 (2008) 3181–3197.
- [13] C.J. Davies, G.A. Solan, J. Fawcett, Polyhedron 23 (2004) 3105–3114.
- [14] A. Malassa, H. Görls, A. Buchholz, W. Plass, M. Westerhausen, Z. Anorg. Allg. Chem. 632 (2006) 2355–2362.
- [15] D.C. Bradley, M.H. Chisholm, Acc. Chem. Res. 9 (1976) 273–280.
- [16] (a) R. Kempe, Angew. Chem. 112 (2000) 478–504; (b) Angew. Chem. Int. Ed. 39 (2000) 468–493.
- [17] (b) M.F. Lappert, P.P. Power, A.R. Sanger, R.C. Srivastava, Metal and Metalloid Amides. Ellis Horwood, Chichester, 1980; (b) M. Lappert, P. Power, A. Protchenko, A. Seeber, Metal Amide Chemistry. Wiley, Chichester, 2009.
- [18] H. Bürger, U. Wannagat, Monatsh. Chem. 95 (1964) 1099–1102.
- [19] B.D. Murray, P.P. Power, Inorg. Chem. 23 (1984) 4584–4588.
- [20] R.A. Andersen, K. Faegri, J.C. Green, A. Haaland, M.F. Lappert, W.-P. Leung, K. Rypdal, Inorg. Chem. 27 (1988) 1782–1786.
- [21] M.M. Olmstead, P.P. Power, S.C. Shoner, Inorg. Chem. 30 (1991) 2547–2551.
- [22] H. Bürger, U. Wannagat, Monatsh. Chem. 94 (1963) 1007–1012.
- [23] C. Incarvito, M. Lam, B. Rhatigan, A.L. Rheingold, C.J. Qin, A.L. Gavrilova, B. Bosnich, J. Chem. Soc., Dalton Trans. (2001) 3478–3488.
- [24] M.I.D. Holanda, P. Krumholz, H.L. Chum, Inorg. Chem. 15 (1976) 890–893.
- [25] E. Baggio-Saitovitch, M.A. de Paoli, Inorg. Chim. Acta 27 (1978) 15–20.

- [26] B.A. Frazier, P.T. Wolczanski, E.B. Lobkovsky, T.R. Cundari, *J. Am. Chem. Soc.* 131 (2009) 3428–3429.
- [27] M. Westerhausen, A.N. Kneifel, *Inorg. Chem. Commun.* 7 (2004) 763–766.
- [28] M. Westerhausen, A.N. Kneifel, I. Lindner, J. Grčić, H. Nöth, *Z. Naturforsch.* 59b (2004) 161–166.
- [29] C. Koch, A. Malassa, C. Agthe, H. Görls, R. Biedermann, H. Krautscheid, M. Westerhausen, *Z. Anorg. Allg. Chem.* 633 (2007) 375–382.
- [30] (a) H. Bürger, W. Sawodny, U. Wannagat, *J. Organomet. Chem.* 3 (1965) 113–120;  
(b) A. Haaland, K. Hedberg, P.P. Power, *Inorg. Chem.* 23 (1984) 1972–1975;  
(c) I.E. Gümrükçüoğlu, J. Jeffery, M.F. Lappert, J.B. Pedley, A.K. Rai, *J. Organomet. Chem.* 341 (1988) 53–62;  
(d) M. Bochmann, G. Bwembya, K.J. Webb, *Inorg. Synth.* 31 (1997) 24;  
(e) G. Markgraf, H.-W. Lerner, M. Bolte, M. Wagner, *Z. Anorg. Allg. Chem.* 630 (2004) 217–218.
- [31] (a) B. Machelett, *Z. Chem* 16 (1976) 116–117;  
(b) H. Müller, W. Seidel, H. Görls, *J. Organomet. Chem.* 445 (1993) 133–136.
- [32] R.A. Layfield, *Chem. Soc. Rev.* 37 (2008) 1098–1107.
- [33] A.A. Kulkarni, O. Daugulis, *Synthesis* (2009) 4087–4109.
- [34] COLLECT, Data Collection Software; Nonius B.V., Netherlands, 1998.
- [35] Z. Otwinowski, W. Minor, Processing of X-ray diffraction data collected in oscillation mode. in: C.W. . Carter, R.M. Sweet (Eds.), *Methods in Enzymology, Macromolecular Crystallography, Part A*, vol. 276. Academic Press, 1997, pp. 307–326.
- [36] G.M. Sheldrick, *Acta Crystallogr. A*46 (1990) 467–473.
- [37] G.M. Sheldrick, SHELXL-97 (Release 97-2). University of Göttingen, Germany, 1997.